
The Neural Testbed: Evaluating Joint Predictions

Ian Osband*, Zheng Wen, Seyed Mohammad Asghari,
Brendan O'Donoghue, Botao Hao, Dieterich Lawson, Morteza Ibrahimi,
Xiuyuan Lu, Vikranth Dwaracherla, and Benjamin Van Roy
DeepMind, Efficient Agent Team, Mountain View

Abstract

Predictive distributions quantify uncertainties ignored by point estimates. This paper introduces *The Neural Testbed*: an open-source benchmark for controlled and principled evaluation of agents that generate such predictions. Crucially, the testbed assesses agents not only on the quality of their marginal predictions per input, but also on their joint predictions across many inputs. We evaluate a range of agents using a simple neural network data generating process. Our results indicate that some popular Bayesian deep learning agents do not fare well with joint predictions, even when they can produce accurate marginal predictions. We also show that the quality of joint predictions drives performance in downstream decision tasks. We find these results are robust across choice a wide range of generative models, and highlight the practical importance of joint predictions to the community.

1 Introduction

Most work on supervised learning has focused on marginal predictions. Marginal predictions predict one label given one input, but do not model the dependence between multiple predictions. For decision making, it is not enough to have good marginal predictions; the quality of *joint* predictions drives decision performance (Wen et al., 2022). Joint predictions predict multiple labels given multiple inputs, and may capture some correlation between outcomes. This distinction can be particularly important in learning settings where joint predictions allow an agent to distinguish what it knows from what it does not know (Li et al., 2011; Lu et al., 2021).



coin	bias	marginal prediction	joint prediction													
	$\frac{1}{2}$	<table><tr><td>H</td><td>0.5</td></tr><tr><td>T</td><td>0.5</td></tr></table>	H	0.5	T	0.5	<table><tr><td></td><td>H</td><td>T</td></tr><tr><td>H</td><td>0.25</td><td>0.25</td></tr><tr><td>T</td><td>0.25</td><td>0.25</td></tr></table>		H	T	H	0.25	0.25	T	0.25	0.25
H	0.5															
T	0.5															
	H	T														
H	0.25	0.25														
T	0.25	0.25														
	0 or 1	<table><tr><td>H</td><td>0.5</td></tr><tr><td>T</td><td>0.5</td></tr></table>	H	0.5	T	0.5	<table><tr><td></td><td>H</td><td>T</td></tr><tr><td>H</td><td>0.5</td><td>0</td></tr><tr><td>T</td><td>0</td><td>0.5</td></tr></table>		H	T	H	0.5	0	T	0	0.5
H	0.5															
T	0.5															
	H	T														
H	0.5	0														
T	0	0.5														

Figure 1: Two coins with identical marginal predictions, but distinguished by joint predictions.

*Contact iosband@deepmind.com

Figure 1 presents a stylized example designed to highlight the importance of joint predictions in decision making. Consider two coins ‘£’ and ‘\$’ with different *bias*=‘probability of heads’. Coin £ has a known bias of $\frac{1}{2}$, whereas coin \$ has an unknown bias of either 0 or 1, and which are both equally likely. Examining the marginal prediction over a single flip: the two coins present identical outcomes 50:50. However, if we consider the outcome over two successive flips, which can be modeled as a two-by-two grid, then the difference between these coins is evident in their joint predictions. If you want to maximize the cumulative heads through time, then it’s important to know the difference between these two settings. In this case, a learning agent should first choose \$ and then, depending on the outcome of that flip heads/tails, employ a fixed policy of \$/£ forward. Marginal predictions alone cannot drive this sort of policy, since they do not distinguish the two coins (Wen et al., 2022).

Our research is motivated by the grand challenges in artificial intelligence, and the great progress that has been made in deep learning systems (Krizhevsky et al., 2012; Brown et al., 2020). However, as these systems move beyond prediction and towards actually making decisions we have very little understanding of how and where popular deep learning approaches are suitable for joint predictions and hence decision making (Mnih et al., 2015; Silver et al., 2016). To this end, we introduce *The Neural Testbed* as a simple and clear benchmark for evaluating the quality of joint predictions in deep learning systems. This work is meant to be a ‘sanity check’ for popular deep learning approaches in a simple setting, and one that can help guide future research.

The Neural Testbed works by generating random classification problems using a neural-network-based generative process. The testbed splits data into a training set and testing set, allows a deep learning agent to train on the training set, and then evaluates the quality of the predictions on the testing set. It is worth noting that the problem framed by the Testbed is a *computational* one. Optimal performance would be attained by carrying out exact Bayesian inference: given infinite compute time, an agent could calculate the posterior distribution, which maximizes performance. However, due to the complexity of the data generating process, this is infeasible. The agents we study serve as approximate inference algorithms, and we can compare their performance purely through the quality of their predictions, without worrying ‘is XYZ Bayesian?’ (Izmailov et al., 2021).

Figure 2 offers a preview of our results in Section 4, where we compare benchmark approaches to Bayesian deep learning. This plot shows the KL loss when making τ simultaneous predictions. We compare the quality of marginal ($\tau = 1$) and joint ($\tau = 10$) predictions, normalized so that and MLP has loss=1. We see that, after tuning, most Bayesian deep learning approaches do not significantly outperform a single MLP in marginal predictions.

However, once we examine joint predictive distributions of order $\tau = 10$, there is a clear difference in performance among benchmark agents. In particular, some of the most popular benchmark approaches to Bayesian deep learning (**ensemble** (Lakshminarayanan et al., 2017), **dropout** (Gal and Ghahramani, 2016), **bbb** (Blundell et al., 2015)) do not outperform the baseline MLP when evaluated in joint predictions. At the same time, there are other approaches that perform much better in terms of joint predictions in this simple synthetic challenge. We will go on to show that these same agents perform better in decision making, and that these observations are robust to choice of generative model.

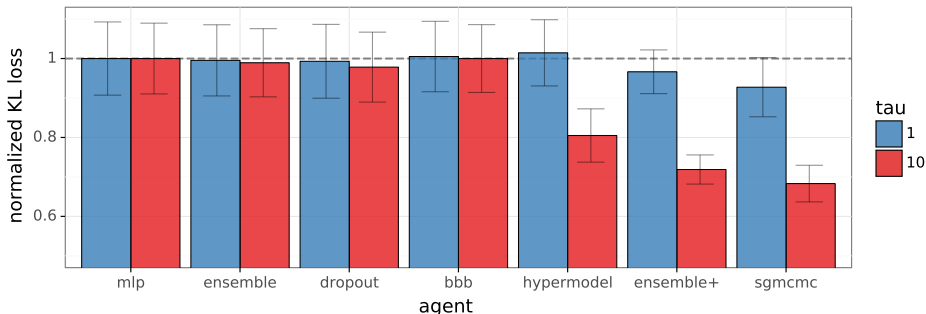


Figure 2: Quality of marginal and joint predictions on Neural Testbed (Section 4.2).

1.1 Key contributions

We introduce *The Neural Testbed*, a simple benchmark for the field that involves making predictions in a neural-network-based generative model. This work helps to bridge theory and practice, and provide an objective metric to assess the quality of approximate posterior inference in neural networks. We are the first paper to propose a concrete evaluation procedure for the quality of joint predictions in neural network classification.

Together with this conceptual contribution, we open-source code in Appendix A. This consists of highly optimized evaluation code, reference agent implementations and automated reproducible analysis. The testbed uses JAX internally (Bradbury et al., 2018), but can be used to evaluate any python agent. We believe that this library will be a major contribution to researchers and, due to its low computational cost, a boon to accessibility.

We use this new benchmark to obtain some important new experimental results. **We discover that several of the most popular approaches to Bayesian deep learning do not perform well at joint prediction**, and highlight this issue to the community. Further, we show that there *are* alternative approaches that *do* perform well in terms of joint prediction. Prior work has suggested that, in theory, the quality of joint predictions can drive decision performance (Wen et al., 2022). In this paper we provide empirical evidence that this effect occurs in practical deep learning systems. **We observe that performance in a neural bandit is highly correlated with performance in joint prediction**, and that it is not significantly correlated with the quality of marginal predictions.

Finally, **we show that the results in this paper are robust to the variations in the data generating model**. Although we focus on a 2-layer ReLU MLP with 50 hidden units for most of our experiments, the results we obtain are highly correlated across a wide range of alternative activation functions or network widths. This robustness supports the view that the field should be aware of these issues in joint prediction, and may help to stimulate future research in this area. Follow-up work has gone on to show that these results also carry over to challenge datasets popular in the community (Osband et al., 2022).

1.2 Related work

There is a rich literature around uncertainty estimation in deep learning. Much of this work has focused on agent development, with a wide variety of approaches including variational inference (Blundell et al., 2015), dropout (Gal and Ghahramani, 2016), ensembles (Osband and Van Roy, 2015; Lakshminarayanan et al., 2017), and MCMC (Welling and Teh, 2011; Hoffman et al., 2014). However, even when approaches become popular within particular research communities, there are still significant disagreements over the quality of the resultant uncertainty estimates (Osband, 2016; Hron et al., 2017).

Bayesian deep learning has largely relied on benchmark problems to guide agent development and measure agent progress. These typically include classic deep learning datasets but supplement the usual goal of classification accuracy to include an evaluation of the probabilistic predictions via negative log likelihood (NLL) and expected calibration error (ECE) (Nado et al., 2021). More recently, several efforts have been made to supplement these datasets with challenges tailored towards Bayesian deep learning, and explicit Bayesian inference (Wilson et al., 2021). This literature has largely focused on evaluating marginal predictions, paired with evaluation on downstream tasks (Riquelme et al., 2018). Our work is motivated by the importance of *joint* predictions in driving good performance in sequential decisions (Wen et al., 2022). We share motivation with the work of Wang et al. (2021), but show that directly measuring joint likelihoods can provide new information beyond marginals. Follow up work has built upon the research in our paper, to extend the analysis of joint distributions to higher-order joint distributions, and empirical datasets (Osband et al., 2022).

2 Evaluating predictive distributions

In this section, we introduce notation for the standard supervised learning we consider as well as our evaluation metric: KL-loss. We review the distinction between marginal and joint predictions, and numerical schemes to estimate KL divergence via Monte Carlo sampling.

Algorithm 1 KL-Loss Estimation

```

for  $j = 1, 2, \dots, J$  do
  sample environment and training data
  train agent on training data
  for  $n = 1, 2, \dots, N$  do
    sample  $\tau$  test data pairs
    compute environment likelihood  $p_{j,n}$ 
    compute agent likelihood  $\hat{p}_{j,n}$ 
  end for
end for
return  $\frac{1}{JN} \sum_{j=1}^J \sum_{n=1}^N \log(p_{j,n}/\hat{p}_{j,n})$ 

```

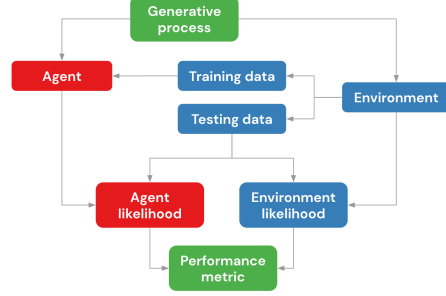


Figure 3: The Neural Testbed

2.1 Environment and predictions

Consider a sequence of pairs $((X_t, Y_{t+1}) : t = 0, 1, 2, \dots)$, where each X_t is a feature vector and each Y_{t+1} is its target label. Each target label Y_{t+1} is produced by an *environment* \mathcal{E} , which we formally take to be a conditional distribution $\mathcal{E}(\cdot|X_t)$. The environment \mathcal{E} is a random variable; this reflects the agent’s uncertainty about how labels are generated. Note that $\mathbb{P}(Y_{t+1} \in \cdot | \mathcal{E}, X_t) = \mathcal{E}(\cdot|X_t)$ and $\mathbb{P}(Y_{t+1} \in \cdot | X_t) = \mathbb{E}[\mathcal{E}(\cdot|X_t)|X_t]$.

We consider an agent that learns about the environment from training data $\mathcal{D}_T \equiv ((X_t, Y_{t+1}) : t = 0, 1, \dots, T-1)$. After training, the agent predicts testing class labels $Y_{T+1:T+\tau} \equiv (Y_{T+1}, \dots, Y_{T+\tau})$ from unlabeled feature vectors $X_{T:T+\tau-1} \equiv (X_T, \dots, X_{T+\tau-1})$.

We describe the agent’s predictions in terms of a generative model, parameterized by a vector θ_T that the agent learns from the training data \mathcal{D}_T . For any inputs $X_{T:T+\tau-1}$, θ_T determines a predictive distribution, which could be used to sample imagined outcomes $\hat{Y}_{T+1:T+\tau}$. Hence, the agents τ^{th} -order predictive distribution is given by

$$\hat{P}_{T+1:T+\tau} = \mathbb{P}(\hat{Y}_{T+1:T+\tau} \in \cdot | \theta_T, X_{T:T+\tau-1}),$$

which represents an approximation to what would be obtained by conditioning on the environment:

$$P_{T+1:T+\tau}^* = \mathbb{P}(Y_{T+1:T+\tau} \in \cdot | \mathcal{E}, X_{T:T+\tau-1}).$$

If $\tau = 1$, this represents a marginal prediction; that is a prediction of a label for a single input. For $\tau > 1$, this is a joint prediction over labels for τ different inputs.

2.2 Kullback–Leibler loss

We use expected KL-loss to quantify the error between an agent’s predictive distribution $\hat{P}_{T+1:T+\tau}$ and the prescient prediction $P_{T+1:T+\tau}^*$ that would be made given full knowledge of the environment:

$$\mathbf{d}_{\text{KL}}^\tau = \mathbb{E}[\mathbf{d}_{\text{KL}}(P_{T+1:T+\tau}^* \| \hat{P}_{T+1:T+\tau})]. \quad (1)$$

The expectation is taken over all random variables, including the environment \mathcal{E} , the parameters θ_T , $X_{T:T+\tau-1}$, and $Y_{T+1:T+\tau}$. Note that $\mathbf{d}_{\text{KL}}^\tau$ is equivalent to the widely used notion of cross-entropy loss, though offset by a quantity that is independent of θ_T .

In contexts we will consider, it is not possible to compute $\mathbf{d}_{\text{KL}}^\tau$ exactly. As such, we will approximate $\mathbf{d}_{\text{KL}}^\tau$ via Monte Carlo simulation, as described by Algorithm 1. First, a set of environments is sampled. Then, for each sampled environment, a training dataset is sampled. For sampled environment and corresponding training data set, the agent is re-initialized, trained, and then tested on N independent test data τ -samples. Note that each test data τ -sample includes τ data pairs. For each test data τ -sample, the likelihood of the environment $p_{j,n}$ is computed exactly, but that of the agent’s predictive distribution is approximated via another Monte Carlo simulation, and we use $\hat{p}_{j,n}$ to denote this approximation. The estimate of $\mathbf{d}_{\text{KL}}^\tau$ is taken to be the sample mean of these log-likelihood ratios.

3 The Neural Testbed

In this section we introduce the Neural Testbed. We believe that a simple, clear and accessible testbed can provide significant value to community. We provide a high-level overview of the open-source code which we release in Appendix A. We then provide more details on the underlying generative model, together with an extensive selection of benchmark agents that we have tuned to perform well in this setting.

3.1 Synthetic data generating processes

By data generating process, we do not mean only the conditional distribution of data pairs $(X_t, Y_{t+1})|\mathcal{E}$ but also the distribution of the environment \mathcal{E} . The Testbed considers 2-dimensional inputs and binary classification problems. The logits are sampled from a 2-hidden-layer ReLU MLP with (50,50) hidden units and Xavier initialization (Glorot and Bengio, 2010). We choose this process to be maximally simple and canonical in the deep learning world. However, we will go on to show that the key findings of this paper are not particularly sensitive to the exact choice of generative model.

The Neural Testbed estimates KL-loss, with $\tau \in \{1, 10\}$, for three temperature settings and several training dataset sizes. The temperature ρ controls the signal to noise ratio as the class probabilities are given by $\text{softmax}(\text{logits}/\rho)$. For each value of τ , the KL-losses are averaged to produce an aggregate performance measure. Further details concerning data generation and agent evaluation are offered in Appendix B.

3.2 Why do we need a synthetic testbed?

The Neural Testbed is designed to be a maximally simple problem that investigates the key properties of uncertainty modeling in deep learning. Progress in deep learning has been driven both by challenge datasets that stretch agent capabilities (Deng et al., 2009; Krizhevsky et al., 2012), together with foundational work that builds understanding (Bartlett et al., 2021). In this work, we provide a benchmark designed to improve our *understanding* of probabilistic predictions beyond marginals. Doing well in the testbed is not necessarily an impressive grand success in AI, although doing poorly in such a simple setting may reveal fundamental flaws in algorithm design.

A key property of the testbed is that it is specified by a probabilistic model, rather than a finite collection of datasets. Benchmarks that rank performance on datasets are vulnerable to overfitting through iterative hill-climbing on the data included in the benchmark (Russo and Zou, 2016), which may not generalize to data outside of the benchmark (Recht et al., 2018). In contrast, access to a generative model means that we can produce an unlimited amount of testing data from our problem of interest. We can avoid the dangers of overfitting to any specific choices of benchmark dataset simply by generating more samples.

3.3 Benchmark agents

Table 1 lists agents that we study and compare as well as hyperparameters that we tune. In our experiments, we optimize these hyperparameters via grid search. Our implementations, which aim to match ‘canonical’ versions, are available in Appendix A.

In addition to these agent implementations, our open-source offerings include all the evaluation code to reproduce the results of this paper. Our experiments make extensive use of parallel computation to facilitate hyperparameter sweeps. Nevertheless, the overall computational cost is relatively low by modern deep learning standards and relies only on standard CPUs. For reference, evaluating the `mlp` agent across all the problems in our testbed requires less than 3 CPU-hours. We view our open-source effort as a substantial contribution of this work.

4 Results

We evaluate the benchmark agents of Section 3.3 across the Neural Testbed. We begin with an analysis of marginal predictions where, after agent tuning, all approaches are able to make reasonably good predictions. However, when we examine *joint* predictions we find that agent performance can vary drastically, even for well-tuned agents. If an agent cannot

Table 1: Summary of benchmark agents, full details in Appendix C.

agent	description	hyperparameters
mlp	Vanilla MLP	L_2 decay
ensemble	‘Deep Ensemble’ (Lakshminarayanan et al., 2017)	L_2 decay, ensemble size
dropout	Dropout (Gal and Ghahramani, 2016)	L_2 decay, network, dropout rate
bbb	Bayes by Backprop (Blundell et al., 2015)	prior mixture, network, early stopping
hypermodel	Hypermodel (Dwaracherla et al., 2020)	L_2 decay, prior, bootstrap, index dimension
ensemble+	Ensemble + prior functions (Osband et al., 2018)	L_2 decay, ensemble size, prior scale, bootstrap
sgmcmc	Stochastic Langevin MCMC (Welling and Teh, 2011)	learning rate, prior, momentum

output accurate joint predictions in the testbed, we should question if we expect that same agent to perform better other settings. These results provide significant new insights to the the design of effective learning agents, and are a major contribution of this paper.

4.1 Performance in marginal predictions

We begin our evaluation of benchmark approaches to Bayesian deep learning in marginal predictions ($\tau = 1$). One of the first questions one might consider is whether the generative model as outlined in Section 3.1 represents a meaningful challenge for deep learning systems. Figure 4 compares the performance of naive uniform class probabilities, logistic regression, and a tuned 2-layer MLP. This simple comparison demonstrates that the Neural Testbed is not trivially solved by agents without deep learning architectures.

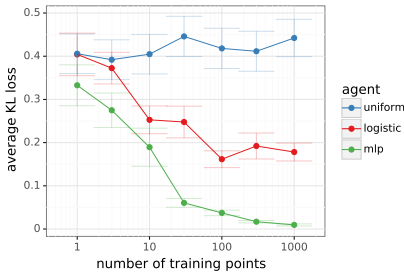


Figure 4: Performance with growing data.

AGENT	ACCURACY	ECE	\mathbf{d}_{KL}^1	$\mathbf{d}_{\text{KL}}^{10}$
MLP	0.793	0.078	0.129	1.367
ENSEMBLE	0.792	0.079	0.128	1.356
DROPOUT	0.793	0.080	0.128	1.347
BBB	0.792	0.079	0.129	1.375
HYPERMODEL	0.793	0.081	0.130	1.107
ENSEMBLE+	0.790	0.085	0.129	1.015
SGMCMC	0.796	0.082	0.122	0.947

Table 2: Agent performance, deviation from MLP greater than 2 stderr in bold.

Marginal predictions have been the focus of the Bayesian deep learning literature. Despite this focus, Figure 2 shows that none of the benchmark methods significantly outperform a well-tuned MLP baseline in terms of \mathbf{d}_{KL}^1 . This observation is mirrored when we examine the average classification accuracy *and* expected calibration error (ECE) across the testbed (Table 2). These results are different from the empirical observations in other challenge datasets, where much agent development has focused on improving ECE, and present an interesting new observation in the Bayesian deep learning literature (Nado et al., 2021). We have two main hypothesis for this discrepancy. First, our agents are tuned for $\mathbf{d}_{\text{KL}}^{\text{agg}} = \mathbf{d}_{\text{KL}}^1 + \frac{1}{10}\mathbf{d}_{\text{KL}}^{10}$, not ECE (see Appendix C). Second, the generative model of Section 3.1 matches the agent architecture, with inputs sampled i.i.d. $N(0, I)$. Investigating the conditions in which these results hold more generally is an exciting area for future research.

4.2 Performance beyond marginals

One of the key contributions of this paper is to evaluate predictive distributions beyond marginals. Figure 2 shows that **sgmcmc** is the top-performing agent overall. This should be reassuring to the Bayesian deep learning community and beyond. In the limit of large compute this agent should recover the ‘gold-standard’ of Bayesian inference, and it does indeed perform best (Welling and Teh, 2011). However, some of the most popular approaches in this field (**ensemble**, **dropout**) do not actually provide good approximations to the predictive distributions of order $\tau = 10$. In fact, we even see that **ensemble+** and **hypermodels** can provide much better approximations to the Bayesian posterior than ‘fully Bayesian’ VI approaches like **bbb** (Wilson and Izmailov, 2020). We note too that while **sgmcmc** performs best, it also requires orders of magnitude more computation than competitive methods even in this toy setting (see Appendix D.3). As we scale to more complex environments, it may therefore be worthwhile to consider alternative approaches.

To see where some agents are able to outperform, we compare **ensemble** and **ensemble+** under the medium SNR regime. These agents are identical, except for the addition of a randomized prior function (Osband et al., 2018). Figure 5 shows that, although these methods perform similarly in the quality of their marginal predictions ($\tau = 1$), the addition of a prior function greatly improves the quality of joint predictive distributions ($\tau = 10$) in the low data regime. Note that, since the testbed considers 2D inputs, 100 training points may already be considered as in the high data regime. Figure 6 provides some insight for how this benefit scales with the order τ of the predictive distribution. We can see a clear trend that as τ increases so does the separation between agents **ensemble** and **ensemble+**. For more intuition on *how* prior functions are able to drive this benefit, see Appendix D.1.

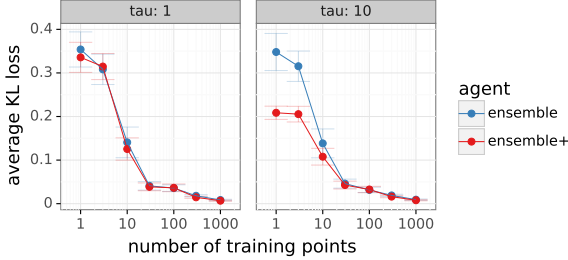


Figure 5: Prior functions help with joint predictions.

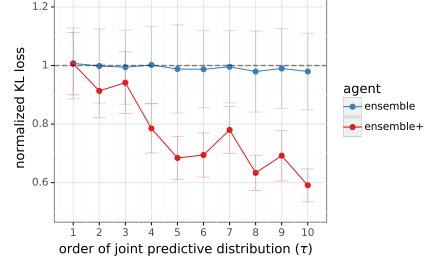


Figure 6: Benefit grows with τ .

5 Sequential decisions

In this section, we will form a sequential decision problem based on the Neural Testbed, and show that it is the quality in *joint* predictions that is essential to driving good performance in sequential decision making. Further, we show that the insights gained from the simple 2D Neural Testbed can extend to high-dimensional decision problems.

5.1 Neural bandit

We use the generative model of the Neural Testbed to define a class of bandit problems (Gittins, 1979). First, we sample a set of N actions $\mathcal{X} = \{x_1, \dots, x_N\}$ i.i.d. from a d -dimensional standard normal distribution. We then sample an environment \mathcal{E} , which specifies the conditional probability $\mathcal{E}(Y_{t+1} \in \cdot | X_t)$, according to the class of generative models described in Section 3.1. We pick the temperature, which controls the SNR, to be 0.1. At each timestep t , an agent selects an action $X_t \in \mathcal{X}$ and receives a reward $R_{t+1} = Y_{t+1}$. Let $\bar{R}_x = \mathbb{E}[R_{t+1} | \mathcal{E}, X_t = x]$ denote the expected reward of action x conditioned on the environment, and let $X_* = \arg \max_{x \in \mathcal{X}} \bar{R}_x$ denote the optimal action. We assess agent performance through $\text{regret}(T) := \sum_{t=0}^{T-1} \mathbb{E}[\bar{R}_{X_*} - \bar{R}_{X_t}]$, which measures the shortfall in expected cumulative rewards relative to an optimal decision maker.

We evaluate the testbed agents on these bandit problems through actions selected by Thompson sampling, varying only the posterior predictive distributions that TS samples from. A TS agent requires an approximate posterior distribution over the environment, which is supplied by the testbed agents. At each timestep, TS samples an environment from the approximate posterior and selects an action that optimizes for the sampled environment (Thompson, 1933; Russo et al., 2018). A complete algorithm is presented in Appendix E.

5.2 Agent performance

We present empirical results of testbed agents on these random bandit problems with $N = 1000$ actions drawn from a $d = 50$ dimensional space. Figure 7 shows the average regret through time for each of the agents as selected by the Neural Testbed, averaged over 20 random seeds.² We can see that for each learning agent, the quality of decisions improves through time. However, the quality of decisions is greatly affected by the choice of agent.

²We omit **sgmcmc** as the computational demands are several orders of magnitude too large to consider in online learning.

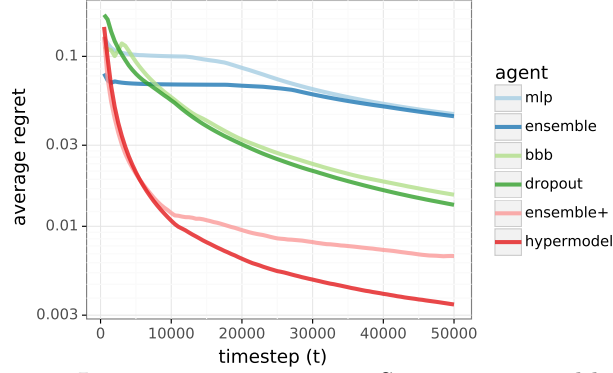


Figure 7: Learning agent impacts TS regret in neural bandits.

To investigate the relationship between predictions and decisions we repeat the experiment of Figure 7 with 10 independent random initializations over all the testbed and bandit problems. We then empirically investigate the correlation between \mathbf{d}_{KL}^T and total regret at $T = 50,000$ for both $\tau = 1$ and $\tau = 10$. We use bootstrap sampling to estimate confidence intervals on the correlation coefficient on a logarithmic scale at the 5th and 95th percentiles. Figures 8 and 9 support our claim that performance in $\mathbf{d}_{\text{KL}}^{10}$ is highly correlated with performance in sequential decision problems, whereas correlation to marginals is not significant. We would not expect a perfect correlation as the particular TS action selection strategy may introduce confounding factors, together with natural variability in seeds.

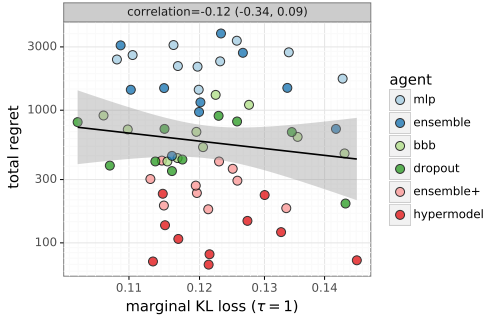


Figure 8: Testbed marginal performance is not significantly correlated with regret.

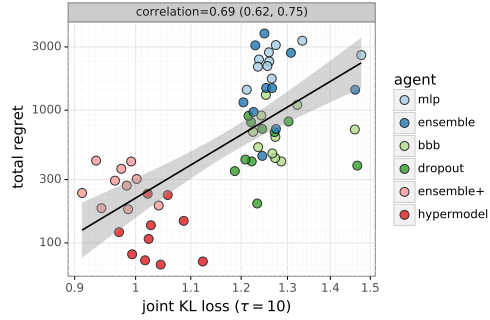


Figure 9: Testbed joint performance is highly correlated with regret.

6 Robustness of generative model

The experiments of Sections 4 and 5 are all performed with the generative model as described in Section 3.1. One natural concern is that these results might be sensitive to this choice of model, and so be less transferable to general deep learning research. In this section we repeat these analyses under different generative models. We find that the quality of *joint* predictions and bandit performance is extremely robust across choice of generative models.

For these experiments we take the tuned agents of Section 4 and then evaluate these agents under different generative models. Whereas these agent hyperparameters were tuned for the 2-layer ReLU MLP with 50-50 hidden units, we will also evaluate these agents over alternative environments varying:

- **activation**=[tanh, swish, sigmoid, selu, relu, leaky relu, gelu] (Figure 10).
- **hidden units**=[5, 10, 20, 50, 100] (Figure 11).

Evaluation for each of these environments \mathcal{E}_i proceeds as before: the agent is trained on data generated by \mathcal{E}_i and then evaluated on the quality of predictions on testing data from \mathcal{E}_i . If the qualitative results under different environments are similar, then we know that our results are somewhat robust to the exact generative model we choose.

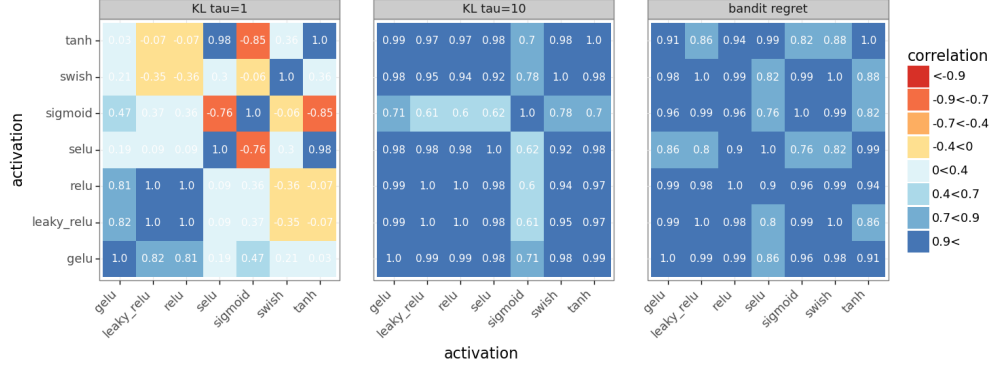


Figure 10: Correlation of agent performance across different activation functions.

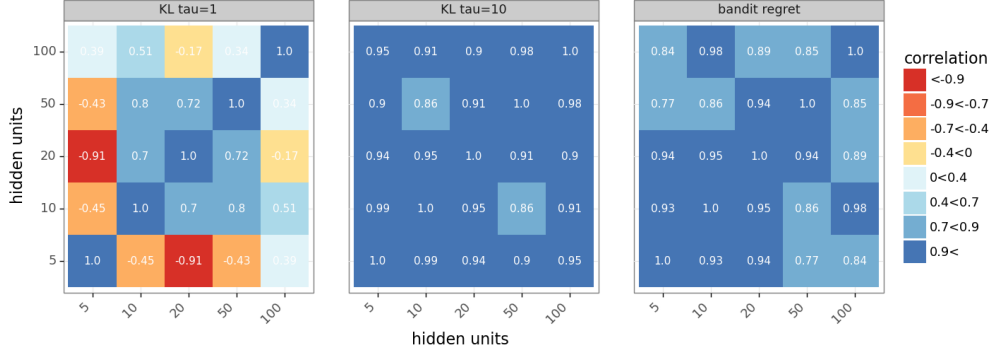


Figure 11: Correlation of agent performance across different hidden units.

Figure 10 and 11 examine the empirical correlation coefficient between the vector of agent evaluations, under the metrics \mathbf{d}_{KL}^1 , $\mathbf{d}_{\text{KL}}^{10}$ and bandit regret. We see that, the marginal evaluations are highly correlated for ‘similar’ generative models (e.g. ReLU and leaky ReLU) but can even be anti-correlated when the models stray too far. However, the correlations are very high across a wide range of generative models when we look at either the quality of joint predictions or the regret in the bandit problems. These results help to build confidence in the key observations we make in this paper. Notably, they suggest that the separation of agents in terms of performance on joint prediction (Figure 2) is not too sensitive to the choice of generative model, and so may hold some wider insight relevant to the community. Follow up work has confirmed that these results are also highly correlated with performance on benchmark datasets (Osband et al., 2022).

7 Conclusion

The Neural Testbed investigates the quality of predictive uncertainty in joint predictions, as well as marginals. With this simple and clear 2D challenge we aim to build understanding that can inform the field’s wider efforts in deep learning. We have shown that results on the testbed can offer new insights to agent development. Further, we establish that the insights gained in the testbed can scale up to complex and high-dimensional decision problems.

Beyond the results in this paper, we believe this work can provide a base for future research:

- Can we design better learning algorithms for joint predictions, as well as marginals?
- Are there analogous results to Figure 2 on large-scale challenge datasets?
- How can effective joint predictions drive better decisions?

We believe that studying these simple testbed problems can help foster interplay between theory and practice, improve accessibility in the field, and complement existing research. We hope that this will accelerate the growth of *understanding* in the field and, ultimately, drive forward the design of better learning agents.

References

- Bartlett, P. L., Montanari, A., and Rakhlin, A. (2021). Deep learning: a statistical viewpoint. *Acta numerica*, 30:87–201.
- Blundell, C., Cornebise, J., Kavukcuoglu, K., and Wierstra, D. (2015). Weight uncertainty in neural network. In *International Conference on Machine Learning*, pages 1613–1622. PMLR.
- Bradbury, J., Frostig, R., Hawkins, P., Johnson, M. J., Leary, C., Maclaurin, D., Necula, G., Paszke, A., VanderPlas, J., Wanderman-Milne, S., and Zhang, Q. (2018). JAX: composable transformations of Python+NumPy programs.
- Brown, T. B., Mann, B., Ryder, N., Subbiah, M., Kaplan, J., Dhariwal, P., Neelakantan, A., Shyam, P., Sastry, G., Askell, A., et al. (2020). Language models are few-shot learners. *arXiv preprint arXiv:2005.14165*.
- Cover, T. and Hart, P. (1967). Nearest neighbor pattern classification. *IEEE transactions on information theory*, 13(1):21–27.
- Deng, J., Dong, W., Socher, R., Li, L.-J., Li, K., and Fei-Fei, L. (2009). Imagenet: A large-scale hierarchical image database. In *2009 IEEE conference on computer vision and pattern recognition*, pages 248–255. Ieee.
- Dwaracherla, V., Lu, X., Ibrahimi, M., Osband, I., Wen, Z., and Van Roy, B. (2020). Hypermodels for exploration. In *International Conference on Learning Representations*.
- Friedman, J. H. (2017). *The elements of statistical learning: Data mining, inference, and prediction*. springer open.
- Gal, Y. and Ghahramani, Z. (2016). Dropout as a Bayesian approximation: Representing model uncertainty in deep learning. In *International Conference on Machine Learning*.
- Gittins, J. C. (1979). Bandit processes and dynamic allocation indices. *Journal of the Royal Statistical Society: Series B (Methodological)*, 41(2):148–164.
- Glorot, X. and Bengio, Y. (2010). Understanding the difficulty of training deep feedforward neural networks. In *Proceedings of the 13th international conference on artificial intelligence and statistics*, pages 249–256.
- He, B., Lakshminarayanan, B., and Teh, Y. W. (2020). Bayesian deep ensembles via the neural tangent kernel. In Larochelle, H., Ranzato, M., Hadsell, R., Balcan, M., and Lin, H., editors, *Advances in Neural Information Processing Systems*, volume 33, pages 1010–1022. Curran Associates, Inc.
- Hoffman, M. D., Gelman, A., et al. (2014). The no-u-turn sampler: adaptively setting path lengths in Hamiltonian Monte Carlo. *J. Mach. Learn. Res.*, 15(1):1593–1623.
- Hron, J., Matthews, A. G. d. G., and Ghahramani, Z. (2017). Variational Gaussian dropout is not Bayesian. *arXiv preprint arXiv:1711.02989*.
- Izmailov, P., Vikram, S., Hoffman, M. D., and Wilson, A. G. (2021). What are Bayesian neural network posteriors really like? *arXiv preprint arXiv:2104.14421*.
- Krizhevsky, A., Sutskever, I., and Hinton, G. E. (2012). Imagenet classification with deep convolutional neural networks. In *Advances in Neural Information Processing Systems 25*, pages 1097–1105.
- Lakshminarayanan, B., Pritzel, A., and Blundell, C. (2017). Simple and scalable predictive uncertainty estimation using deep ensembles. In *Advances in Neural Information Processing Systems*, pages 6405–6416.
- Li, L., Littman, M. L., Walsh, T. J., and Strehl, A. L. (2011). Knows what it knows: a framework for self-aware learning. *Machine learning*, 82(3):399–443.
- Lu, X., Van Roy, B., Dwaracherla, V., Ibrahimi, M., Osband, I., and Wen, Z. (2021). Reinforcement learning, bit by bit. *arXiv preprint arXiv:2103.04047*.
- Mnih, V., Kavukcuoglu, K., Silver, D., Rusu, A. A., Veness, J., Bellemare, M. G., Graves, A., Riedmiller, M., Fidjeland, A. K., Ostrovski, G., et al. (2015). Human-level Control through Deep Reinforcement Learning. *Nature*, 518(7540):529–533.

- Murphy, K. P. (2012). *Machine Learning: A Probabilistic Perspective*. MIT Press.
- Nado, Z., Band, N., Collier, M., Djolonga, J., Dusenberry, M., Farquhar, S., Filos, A., Havasi, M., Jenatton, R., Jerfel, G., Liu, J., Mariet, Z., Nixon, J., Padhy, S., Ren, J., Rudner, T., Wen, Y., Wenzel, F., Murphy, K., Sculley, D., Lakshminarayanan, B., Snoek, J., Gal, Y., and Tran, D. (2021). Uncertainty Baselines: Benchmarks for uncertainty & robustness in deep learning. *arXiv preprint arXiv:2106.04015*.
- Osband, I. (2016). Risk versus uncertainty in deep learning: Bayes, bootstrap and the dangers of dropout. In *NIPS Workshop on Bayesian Deep Learning*, volume 192.
- Osband, I., Aslanides, J., and Cassirer, A. (2018). Randomized prior functions for deep reinforcement learning. In Bengio, S., Wallach, H., Larochelle, H., Grauman, K., Cesa-Bianchi, N., and Garnett, R., editors, *Advances in Neural Information Processing Systems 31*, pages 8617–8629. Curran Associates, Inc.
- Osband, I. and Van Roy, B. (2015). Bootstrapped Thompson sampling and deep exploration. *arXiv preprint arXiv:1507.00300*.
- Osband, I., Wen, Z., Asghari, M., Ibrahimi, M., Lu, X., and Van Roy, B. (2021). Epistemic neural networks. *arXiv preprint arXiv:2107.08924*.
- Osband, I., Wen, Z., Asghari, S. M., Dwaracherla, V., Lu, X., and Van Roy, B. (2022). Evaluating high-order predictive distributions in deep learning.
- Pedregosa, F., Varoquaux, G., Gramfort, A., Michel, V., Thirion, B., Grisel, O., Blondel, M., Prettenhofer, P., Weiss, R., Dubourg, V., Vanderplas, J., Passos, A., Cournapeau, D., Brucher, M., Perrot, M., and Duchesnay, E. (2011). Scikit-learn: Machine learning in Python. *Journal of Machine Learning Research*, 12:2825–2830.
- Rasmussen, C. E. (2003). Gaussian processes in machine learning. In *Summer school on machine learning*, pages 63–71. Springer.
- Recht, B., Roelofs, R., Schmidt, L., and Shankar, V. (2018). Do cifar-10 classifiers generalize to cifar-10? *arXiv preprint arXiv:1806.00451*.
- Rezende, D. and Mohamed, S. (2015). Variational inference with normalizing flows. In *International conference on machine learning*, pages 1530–1538. PMLR.
- Riquelme, C., Tucker, G., and Snoek, J. (2018). Deep bayesian bandits showdown: An empirical comparison of bayesian deep networks for thompson sampling. *arXiv preprint arXiv:1802.09127*.
- Russo, D. and Zou, J. (2016). Controlling bias in adaptive data analysis using information theory. In *Artificial Intelligence and Statistics*, pages 1232–1240. PMLR.
- Russo, D. J., Van Roy, B., Kazerouni, A., Osband, I., and Wen, Z. (2018). A tutorial on Thompson sampling. *Found. Trends Mach. Learn.*, 11(1):1–96.
- Schölkopf, B. and Smola, A. J. (2018). *Learning with kernels: Support vector machines, regularization, optimization, and beyond*. MIT press.
- Silver, D., Huang, A., Maddison, C. J., Guez, A., Sifre, L., Van Den Driessche, G., Schrittwieser, J., Antonoglou, I., Panneershelvam, V., Lanctot, M., et al. (2016). Mastering the game of go with deep neural networks and tree search. *Nature*, 529(7587):484–489.
- Sun, S., Zhang, G., Shi, J., and Grosse, R. (2019). Functional variational Bayesian neural networks. *arXiv preprint arXiv:1903.05779*.
- Thompson, W. R. (1933). On the likelihood that one unknown probability exceeds another in view of the evidence of two samples. *Biometrika*, 25(3/4):285–294.
- Wang, C., Sun, S., and Grosse, R. (2021). Beyond marginal uncertainty: How accurately can Bayesian regression models estimate posterior predictive correlations? In *International Conference on Artificial Intelligence and Statistics*, pages 2476–2484. PMLR.
- Welling, M. and Teh, Y. W. (2011). Bayesian learning via stochastic gradient Langevin dynamics. In *Proceedings of the 28th international conference on machine learning (ICML-11)*, pages 681–688. Citeseer.

- Wen, Z., Osband, I., Qin, C., Lu, X., Ibrahimi, M., Dwaracherla, V., Asghari, M., and Van Roy, B. (2022). From predictions to decisions: The importance of joint predictive distributions.
- Wilson, A. G. and Izmailov, P. (2020). Bayesian deep learning and a probabilistic perspective of generalization. *arXiv preprint arXiv:2002.08791*.
- Wilson, A. G., Izmailov, P., Hoffman, M. D., Gal, Y., Li, Y., Pradier, M. F., Vikram, S., Foong, A., Lotfi, S., and Farquhar, S. (2021). Evaluating approximate inference in Bayesian deep learning.
- Woodbury, M. A. (1950). *Inverting modified matrices*. Statistical Research Group.

A Open source code

This section is meant to give an overview of our opensource code. Together with our paper submission we include a link to anonymous github repository.

- **neural_testbed**: https://github.com/deepmind/neural_testbed

Together with this git repo, we include a ‘tutorial colab’ – a Jupyter notebooks that can be run in the browser without requiring any local installation at `neural_testbed/tutorial.ipynb`. Our library is written in Python, and relies heavily on JAX for scientific computing (Bradbury et al., 2018). We view this open-source effort as a major contribution of our paper.

B Testbed Pseudocode

We present the testbed pseudocode in this section. Specifically, Algorithm 2 is the pseudocode for our neural testbed, and Algorithm 3 is an approach to estimate the likelihood of a test data τ -sample conditioned on an agent’s belief, based on the standard Monte-Carlo estimation. The presented testbed pseudocode works for any prior $\mathbb{P}(\mathcal{E} \in \cdot)$ over the environment and any input distribution P_X , including the ones described in Section 3.1. We also release full code and implementations in Appendix A.

In addition to presenting the testbed pseudocode, we also explain our choices of experiment parameters in Appendix C. To apply Algorithm 2, we need to specify an input distribution P_X and a prior distribution on the environment $\mathbb{P}(\mathcal{E} \in \cdot)$. Recall from Section 3.1 that we consider binary classification problems with input dimension 2. We choose $P_X = N(0, I)$, and we consider three environment priors distinguished by a temperature parameter that controls the signal-to-noise ratio (SNR) regime. We sweep over temperatures in $\{0.01, 0.1, 0.5\}$. The prior distribution $\mathbb{P}(\mathcal{E} \in \cdot)$ is induced by a distribution over MLPs with 2 hidden layers and ReLU activation. The MLP is distributed according to standard Xavier initialization, except that biases in the first layer are drawn from $N(0, \frac{1}{2})$. The MLP outputs two units, which are divided by the temperature parameter and passed through the softmax function to produce class probabilities. The implementation of this generative model is in our open source code under the path `/generative/factories.py`.

We now describe the other parameters we use in the Testbed. In Algorithm 2, we pick the order of predictive distributions $\tau \in \{1, 10\}$, training dataset size $T \in \{1, 3, 10, 30, 100, 300, 1000\}$, number of sampled problems $J = 10$, and number of testing data τ -samples $N = 1000$. To apply Algorithm 3, we sample $M = 1000$ models from the agent.

C Agents

In this section, we describe the benchmark agents in Section 3.3 and the choice of various hyperparameters used in the implementation of these agents. The list of agents include MLP, ensemble, dropout, Bayes by backprop, stochastic Langevin MCMC, ensemble+ and hypermodel. We will also include other agents such as KNN, random forest, and deep kernel, but the performance of these agents was worse than the other benchmark agents, so we chose not to include them in the comparison in Section 4. In each case, we attempt to match the “canonical” implementation. The complete implementation of these agents including the hyperparameter sweeps used for the Testbed are available in Appendix A. We make use of the Epistemic Neural Networks notation from (Osband et al., 2021) in our code. We set the default hyperparameters of each agent to be the ones that minimize the aggregated KL score $\mathbf{d}_{\text{KL}}^{\text{agg}} = \mathbf{d}_{\text{KL}}^1 + \frac{1}{10} \mathbf{d}_{\text{KL}}^{10}$.

C.1 MLP

The `mlp` agent learns a 2-layer MLP with 50 hidden units in each layer by minimizing the cross-entropy loss with L_2 weight regularization. The L_2 weight decay scale is chosen either to be $\lambda \frac{1}{T}$ or $\lambda \frac{d\sqrt{\beta}}{T}$, where d is the input dimension, β is the temperature of the generative process and

Algorithm 2 Neural Testbed

Require: the testbed requires the following inputs

1. prior distribution over the environment $\mathbb{P}(\mathcal{E} \in \cdot)$, input distribution P_X
2. agent f_θ
3. number of training data T , test distribution order τ
4. number of sampled problems J , number of test data samples N
5. parameters for agent likelihood estimation, as is specified in Algorithm 3

for $j = 1, 2, \dots, J$ **do**

Step 1: sample environment and training data

1. sample environment $\mathcal{E} \sim \mathbb{P}(\mathcal{E} \in \cdot)$
2. sample T inputs X_0, X_1, \dots, X_{T-1} i.i.d. from P_X
3. sample the training labels Y_1, \dots, Y_T conditionally i.i.d. as

$$Y_{t+1} \sim \mathbb{P}(Y \in \cdot | \mathcal{E}, X = X_t) \quad \forall t = 0, 1, \dots, T-1$$

4. choose the training dataset as $\mathcal{D}_T = \{(X_t, Y_{t+1}), t = 0, \dots, T-1\}$

Step 2: train agent

train agent f_{θ_T} based on training dataset \mathcal{D}_T

Step 3: compute likelihoods

for $n = 1, 2, \dots, N$ **do**

1. sample $X_T^{(n)}, \dots, X_{T+\tau-1}^{(n)}$ i.i.d. from P_X
2. generate $Y_{T+1}^{(n)}, \dots, Y_{T+\tau}^{(n)}$ conditionally independently as

$$Y_{t+1}^{(n)} \sim \mathbb{P}(Y \in \cdot | \mathcal{E}, X = X_t^{(n)}) \quad \forall t = T, T+1, \dots, T+\tau-1$$

3. compute the likelihood under the environment \mathcal{E} as

$$p_{j,n} = \mathbb{P}(Y_{T+1:T+\tau}^{(n)} | \mathcal{E}, X_{T:T+\tau-1}^{(n)}) = \prod_{t=T}^{T+\tau-1} \Pr(Y_{t+1}^{(n)} | \mathcal{E}, X_t^{(n)})$$

4. estimate the likelihood conditioned on the agent's belief

$$\hat{p}_{j,n} \approx \mathbb{P}(\hat{Y}_{T+1:T+\tau} = Y_{T+1:T+\tau}^{(n)} | \theta_T, X_{T:T+\tau-1}^{(n)}, Y_{T+1:T+\tau}^{(n)}),$$

based on Algorithm 3 with test data τ -sample $(X_{T:T+\tau-1}^{(n)}, Y_{T+1:T+\tau}^{(n)})$.

end for

return $\frac{1}{JN} \sum_{j=1}^J \sum_{n=1}^N \log(p_{j,n}/\hat{p}_{j,n})$

Algorithm 3 Monte Carlo Estimation of Likelihood of Agent's Belief

Require: the Monte-Carlo estimation requires the following inputs

1. trained agent f_{θ_T} and number of Monte Carlo samples M
2. test data τ -sample $(X_{T:T+\tau-1}, Y_{T+1:T+\tau})$

Step 1: sample M models $\hat{\mathcal{E}}_1, \dots, \hat{\mathcal{E}}_M$ conditionally i.i.d. from $\mathbb{P}(\hat{\mathcal{E}} \in \cdot | \theta_T)$

Step 2: estimate \hat{p} as

$$\hat{p} = \frac{1}{M} \sum_{m=1}^M \mathbb{P}(\hat{Y}_{T+1:T+\tau} = Y_{T+1:T+\tau} | \hat{\mathcal{E}}_m, X_{T:T+\tau-1}, Y_{T+1:T+\tau})$$

return \hat{p}

T is the size of the training dataset. We sweep over $\lambda \in \{10^{-4}, 10^{-3}, 10^{-2}, 10^{-1}, 1, 10, 100\}$. We implement the MLP agent as a special case of a deep ensemble (C.2). The implementation and hyperparameter sweeps for the `mlp` agent can be found in our open source code, as a special case of the `ensemble` agent, under the path `/agents/factories/ensemble.py`.

C.2 Ensemble

We implement the basic “deep ensembles” approach for posterior approximation (Lakshminarayanan et al., 2017). The `ensemble` agent learns an ensemble of MLPs by minimizing the cross-entropy loss with L_2 weight regularization. The only difference between the ensemble members is their independently initialized network weights. We chose the L_2 weight scale to be either $\lambda \frac{1}{MT}$ or $\lambda \frac{d\sqrt{\beta}}{MT}$, where M is the ensemble size, d is the input dimension, β is the temperature of the generative process, and T is the size of the training dataset. We sweep over ensemble size $M \in \{1, 3, 10, 30, 100\}$ and $\lambda \in \{10^{-4}, 10^{-3}, 10^{-2}, 10^{-1}, 1, 10, 100\}$. We find that larger ensembles work better, but this effect is within margin of error after 10 elements. The implementation and hyperparameter sweeps for the `ensemble` agent can be found in our open source code under the path `/agents/factories/ensemble.py`.

C.3 Dropout

We follow Gal and Ghahramani (2016) to build a `dropout` agent for posterior approximation. The agent applies dropout on each layer of a fully connected MLP with ReLU activation and optimizes the network using the cross-entropy loss combined with L_2 weight decay.

The L_2 weight decay scale is chosen to be either $\frac{l^2}{2T}(1 - p_{\text{drop}})$ or $\frac{d\sqrt{\beta}l}{T}$ where p_{drop} is the dropping probability, d is the input dimension, β is the temperature of the data generating process, and T is the size of the training dataset. We sweep over dropout rate $p_{\text{drop}} \in \{0, 0.1, 0.2, 0.3, 0.4, 0.5, 0.6, 0.7, 0.8, 0.9\}$, length scale (used for L_2 weight decay) $l \in \{1, 3, 10\}$, number of neural network layers $\in \{2, 3\}$, and hidden layer size $\in \{50, 100\}$. The implementation and hyperparameter sweeps for the `dropout` agent can be found in our open source code under the path `/agents/factories/dropout.py`.

C.4 Bayes-by-backprop

We follow Blundell et al. (2015) to build a `bbb` agent for posterior approximation. We consider a scale mixture of two zero-mean Gaussian densities as the prior. The Gaussian densities have standard deviations σ_1 and σ_2 , and they are mixed with probabilities p and $1 - p$, respectively. We sweep over $\sigma_1 \in \{0.3, 0.5, 0.7, 1, 2, 4\}$, $\sigma_2 \in \{0.3, 0.5, 0.7\}$, $p \in \{0, 0.5, 1\}$, learning rate $\in \{10^{-3}, 3 \times 10^{-3}\}$, number of training steps $\in \{1000, 2000\}$, number of neural network layers $\in \{2, 3\}$, hidden layer size $\in \{50, 100\}$, and the ratio of the complexity cost to the likelihood cost $\in \{1, d\sqrt{\beta}\}$, where d is the input dimension and β is the temperature of the data generating process. The implementation and hyperparameter sweeps for the `bbb` agent can be found in our open source code under the path `/agents/factories/bbb.py`.

C.5 Stochastic gradient Langevin dynamics

We follow Welling and Teh (2011) to implement a `sgmcmc` agent using stochastic gradient Langevin dynamics (SGLD). We consider two versions of SGLD, one with momentum and other without the momentum. We consider independent Gaussian prior on the neural network parameters where the prior variance is set to be

$$\sigma^2 = \lambda \frac{T}{d\sqrt{\beta}},$$

where λ is a hyperparameter that is swept over $\{0.0025, 0.01, 0.04\}$, d is the input dimension, β is the temperature of the data generating process, and T is the size of the training dataset. We consider a constant learning rate that is swept over $\{10^{-4}, 5 \times 10^{-4}, 10^{-3}, 5 \times 10^{-3}\}$. For SGLD with momentum, the momentum decay term is always set to be 0.9. The number of training batches is 5×10^5 with burn-in time of 10^5 training batches. We save a model every 1000 steps after the burn-in time and use these models as an ensemble during the evaluation.

The implementation and hyperparameter sweeps for the `sgmcmc` agent can be found in our open source code under the path `/agents/factories/sgmcmc.py`.

C.6 Ensemble+

We implement the `ensemble+` agent using deep ensembles with randomized prior functions (Osband et al., 2018) and bootstrap sampling (Osband and Van Roy, 2015). Similar to the vanilla ensemble agent in Section C.2, we consider L_2 weight scale to be either $\lambda \frac{1}{MT}$ or $\lambda \frac{d\sqrt{\beta}}{MT}$. We sweep over ensemble size $M \in \{1, 3, 10, 30, 100\}$ and $\lambda \in \{0.1, 0.3, 1, 3, 10\}$. The randomized prior functions are sampled exactly from the data generating process, and we use a prior scale of $3/\sqrt{\beta}$. In addition, we sweep over bootstrap type (none, exponential, bernoulli).

Note that an ensemble+ agent is obtained by an addition of a prior network to the ensemble agent. We find that the addition of randomized prior functions is crucial for improvement in performance over vanilla deep ensembles in terms of the quality of joint predictions. The implementation and hyperparameter sweeps for the `ensemble+` agent can be found in our open source code under the path `/agents/factories/ensemble_plus.py`.

C.7 Hypermodel

We follow Dwaracherla et al. (2020) to build a `hypermodel` agent for posterior approximation. We consider a linear hypermodel over a 2-layer MLP base model. We sweep over index dimension $\in \{1, 3, 5, 7\}$. The L_2 weight decay is chosen to be either $\lambda \frac{1}{T}$ or $\lambda \frac{d\sqrt{\beta}}{T}$ with $\lambda \in \{0.1, 0.3, 1, 3, 10\}$, where d is the input dimension, β is the temperature of the data generating process, and T is the size of the training dataset. We sweep over bootstrap type (none, exponential, bernoulli). We use an additive prior which is a linear hypermodel prior over an MLP base model, which is similar to the generating process, with number of hidden layers in $\{1, 2\}$, 10 hidden units in each layer, and prior scale from $\{1/\sqrt{\beta}, 1/\beta\}$. The implementation and hyperparameter sweeps for the `hypermodel` agent can be found in our open source code under the path `/agents/factories/hypermodel.py`.

C.8 Non-parametric classifiers

K-nearest neighbors (k-NN) (Cover and Hart, 1967) and random forest classifiers (Friedman, 2017) are simple and cheap off-the-shelf non-parametric baselines (Murphy, 2012; Pedregosa et al., 2011). The ‘uncertainty’ in these classifiers arises merely from the fact that they produce distributions over the labels and as such we do not expect them to perform well relative to more principled approaches. Moreover, these methods have no capacity to model $\mathbf{d}_{\text{KL}}^\tau$ for $\tau > 1$. For the `knn` agent we swept over the number of neighbors $k \in \{1, 5, 10, 30, 50, 100\}$ and the weighting of the contribution of each neighbor as either uniform or based on distance. For the `random_forest` agent we swept over the number of trees in the forest $\{10, 100, 1000\}$, and the splitting criterion which was either the Gini impurity coefficient or the information gain. To prevent infinite values in the KL we truncate the probabilities produced by these classifiers to be in the interval $[0.01, 0.99]$. The implementation and hyperparameter sweeps for the `knn` and `random_forest` agents can be found in our open source code under the paths `/agents/factories/knn.py` and `/agents/factories/random_forest.py`.

C.9 Gaussian process with learned kernel

A neural network takes input $X_t \in \mathcal{X}$ and produces output $Z_{t+1} = W\phi_\theta(X_t) + b \in \mathbf{R}^K$, where $W \in \mathbf{R}^{K \times m}$ is a matrix, $b \in \mathbf{R}^K$ is a bias vector, and $\phi_\theta : \mathcal{X} \rightarrow \mathbf{R}^m$ is the output of the penultimate layer of the neural network. In the case of classification the output Z_{t+1} corresponds to the logits over the class labels, i.e., $\hat{Y}_{t+1} \propto \exp(Z_{t+1})$. The neural network should learn a function that maps the input into a space where the classes are linearly distinguishable. In other words, the mapping that the neural network is learning can be considered a form of *kernel* (Schölkopf and Smola, 2018), where the kernel function $k : \mathcal{X} \times \mathcal{X} \rightarrow \mathbf{R}$ is simply $k(X, X') = \phi_\theta(X)^\top \phi_\theta(X')$. With this in mind, we can take a *trained*

neural network and consider the learned mapping to be the kernel in a Gaussian process (GP) (Rasmussen, 2003), from which we can obtain approximate uncertainty estimates. Concretely, let $\Phi_{0:T-1} \in \mathbf{R}^{T \times m}$ be the matrix corresponding to the $\phi_\theta(X_t)$, $t = 0, \dots, T-1$, vectors stacked row-wise and let $\Phi_{T:T+\tau-1} \in \mathbf{R}^{\tau \times m}$ denote the same quantity for the test set. We can write the kernel function evaluated on the training and test datasets using these matrices. Fix index $i \in \{0, \dots, K-1\}$ to be a particular class index. A GP models the joint distribution over the dataset to be a multi-variate Gaussian, i.e.,

$$\begin{bmatrix} Z_{1:T}^{(i)} \\ Z_{T+1:T+\tau}^{(i)} \end{bmatrix} \sim \mathcal{N} \left(\begin{bmatrix} \mu_{1:T}^{(i)} \\ \mu_{T+1:T+\tau}^{(i)} \end{bmatrix}, \begin{bmatrix} \sigma^2 I + \Phi_{0:T-1} \Phi_{0:T-1}^\top & \Phi_{0:T-1} \Phi_{T:T+\tau-1}^\top \\ \Phi_{T:T+\tau-1} \Phi_{0:T-1}^\top & \Phi_{T:T+\tau-1} \Phi_{T:T+\tau-1}^\top \end{bmatrix} \right)$$

where $\sigma > 0$ models the noise in the training data measurement and $\mu_{1:T}^{(i)}$, $\mu_{T+1:T+\tau}^{(i)}$ are the means under the GP. The conditional distribution is given by

$$P(Z_{T+1:T+\tau}^{(i)} | Z_{1:T}^{(i)}, X_{0:T+\tau-1}) = \mathcal{N}(\mu_{T+1:T+\tau|1:T}^{(i)}, \Sigma_{T+1:T+\tau|1:T})$$

where

$$\Sigma_{T+1:T+\tau|1:T} = \Phi_{T:T+\tau-1} \Phi_{T:T+\tau-1}^\top - \Phi_{T:T+\tau-1} \Phi_{0:T-1}^\top (\sigma^2 I + \Phi_{0:T-1} \Phi_{0:T-1}^\top)^{-1} \Phi_{0:T-1} \Phi_{T:T+\tau-1}^\top.$$

and rather than use the GP to compute $\mu_{T+1:T+\tau|0:T}^{(i)}$ (which would not be possible since we do not observe the true logits) we just take it to be the output of the neural network when evaluated on the test dataset. The matrix being inverted in the expression for $\Sigma_{T+1:T+\tau|0:T}$ has dimension $T \times T$, which may be quite large. We use the Sherman-Morrison-Woodbury identity to rewrite it as follows (Woodbury, 1950)

$$\begin{aligned} \Sigma_{T+1:T+\tau|0:T} &= \Phi_{T:T+\tau-1} (I - \Phi_{0:T-1}^\top (\sigma^2 I + \Phi_{0:T-1} \Phi_{0:T-1}^\top)^{-1} \Phi_{0:T-1}) \Phi_{T:T+\tau-1}^\top \\ &= \sigma^2 \Phi_{T:T+\tau-1} (\sigma^2 I + \Phi_{0:T-1}^\top \Phi_{0:T-1})^{-1} \Phi_{T:T+\tau-1}^\top, \end{aligned}$$

which instead involves the inverse of an $m \times m$ matrix, which may be much smaller. If we perform a Cholesky factorization of positive definite matrix $(\sigma^2 I + \Phi_{0:T-1}^\top \Phi_{0:T-1}) = LL^\top$ then the samples for all logits simultaneously can be drawn by first sampling $\zeta \in \mathbf{R}^{m \times K}$, with each entry drawn IID from $\mathcal{N}(0, 1)$, then forming

$$\hat{Y}_{T+1:T+\tau} \propto \exp(\mu_{T+1:T+\tau|1:T} + \sigma \Phi_{T:T+\tau-1} L^{-\top} \zeta).$$

The implementation and hyperparameter sweeps for the `deep_kernel` agent can be found in our open source code under the path `/agents/factories/deep_kernel.py`.

C.10 Other agents

In our paper we have made a concerted effort to include representative and canonical agents across different families of Bayesian deep learning and adjacent research. In addition to these implementations, we performed extensive tuning to make sure that each agent was given a fair shot. However, with the proliferation of research in this area, it was not possible for us to evaluate all competing approaches. We hope that, by opensourcing the Neural Testbed, we can allow researchers in the field to easily assess and compare their agents to these baselines.

For example, we highlight a few recent pieces of research that might be interesting to evaluate in our setting. Of course, there are many more methods to compare and benchmark. We leave this open as an exciting area for future research.

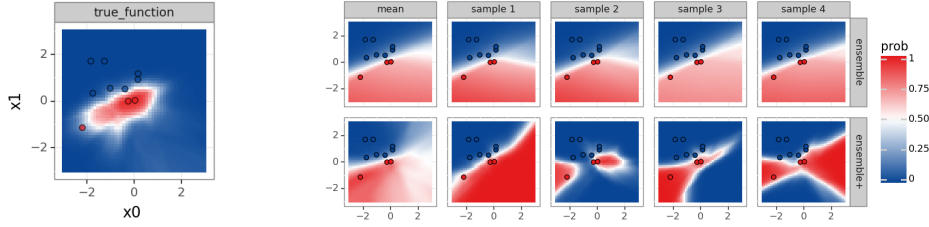
- **Neural Tangent Kernel Prior Functions** (He et al., 2020). Proposes a specific type of prior function in *ensemble+* inspired by connections to the neural tangent kernel.
- **Functional Variational Bayesian Neural Networks** (Sun et al., 2019). Applies variational inference directly to the function outputs, rather than weights like `bbb`.
- **Variational normalizing flows** (Rezende and Mohamed, 2015). Applies variational inference over a more expressive family than `bbb`.
- **No U-Turn Sampler** (Hoffman et al., 2014). Another approach to `sgmcmc` that attempts to compute the posterior directly, computational costs can grow large.

D Testbed results

In this section, we provide the complete results of the performance of benchmark agents on the Testbed, broken down by the temperature setting, which controls the SNR, and the size of the training dataset. We select the best performing agent, based on aggregated score $\mathbf{d}_{\text{KL}}^1 + \mathbf{d}_{\text{KL}}^{10}/10$, within each agent family and plot \mathbf{d}_{KL}^1 and $\mathbf{d}_{\text{KL}}^{10}$ with the performance of an MLP agent as a reference. We also provide a plot comparing the training time of different agents.

D.1 Visualizing ensemble vs ensemble+

Figure 12 provides additional intuition into *how* the randomized prior functions are able to drive improved performance. Figure 12a shows a sampled generative model from our Testbed, with the training data shown in red and blue circles. Figure 12b shows the mean predictions and 4 randomly sampled ensemble members from each agent (top=**ensemble**, bottom=**ensemble+**). We see that, although the agents mostly agree in their mean predictions, **ensemble+** produces more diverse sampled outcomes enabled by the addition of randomized prior functions. In contrast, **ensemble** produces similar samples, which may explain why its performance is close to baseline **mlp** in this setting.



(a) True model. (b) Agent samples: only ensemble+ produces diverse decision boundaries.

Figure 12: Visualization of the predictions of ensemble and ensemble+ agents.

D.2 Performance breakdown

Figures 13 and 14 show the KL estimates evaluated on $\tau = 1$ and $\tau = 10$, respectively. For each agent, for each SNR regime, for each number of training points we plot the average KL estimate from the Testbed. In each plot, we include the “baseline” **mlp** agent as a black dashed line to allow for easy comparison across agents. A detailed description of these benchmark agents can be found in Appendix C.

D.3 Training time

Figure 15 shows a plot comparing the $\mathbf{d}_{\text{KL}}^{10}$ and training time of different agents normalized with that of an MLP. The parameters of each agent are selected to maximize the $\mathbf{d}_{\text{KL}}^{10}$. We can see that **sgmcmc** agent has the best performance, but at the cost of more training time (computation). Both **ensemble+** and **hypermodel** agents have similar performance as **sgmcmc** with lower training time. We trained our agents on CPU only systems.

E Sequential Decision Problems

This section provides supplementary information for the sequential decision problems in Section 5. All of the code necessary to reproduce the experiments is opensourced in the `/bandit/` directory.

E.1 Problem formulation

We consider bandit problems derived from the testbed and evaluate the agents using Algorithm 4 for which we need to specify prior on the environment $\mathbb{P}(\mathcal{E} \in \cdot)$, input distribution P_X , and the number of actions N . We choose input distribution $P_X = \mathcal{N}(0, I_d)$, where d is the input dimension. We sweep over $d \in \{2, 10, 50\}$ and choose the number of actions to be $N = 20d$, i.e., for input dimensions $\{2, 10, 50\}$ we have $\{40, 200, 1000\}$ actions respectively. We use the same prior distribution of environments as in Appendix B with a fixed temperature of 0.1. For each setting, we run for 50,000 time steps ($T = 50,000$) and with 20 random seeds ($J = 20$).

E.2 Agent definition

In Appendix C, we described benchmark agents in our testbed. Among these agents, we use `mlp`, `ensemble`, `dropout`, `bbb`, `ensemble+`, and `hypermodel` agents for sequential decision problems. For all the agents we use the hyper parameters specified by default, in the source code, at the path `/agents/factories/`. The default hyperparameters of each agent correspond to be the ones that minimize the aggregated KL score $\mathbf{d}_{\text{KL}}^{\text{agg}} = \mathbf{d}_{\text{KL}}^1 + \mathbf{d}_{\text{KL}}^{10}/10$. As the agent interacts with the environment, the amount of data the agent has observed keeps growing. Due to this we tune the regularization term based on the number of time steps agent has interacted with the environment. For `mlp`, `ensemble`, `ensemble+`, and `hypermodel` agents we use an L_2 weight decay of $\lambda \frac{2\sqrt{\beta}}{t}$, where β is the temperature, t is the number of the time steps the agent has interacted with the environment, and λ is the default weight scale of the agent. For `dropout` we choose the L_2 weight decay as $\frac{2\sqrt{\beta}l}{t}$, where l is the default length scale used in the dropout agent. For `bbb` we scale the prior term by $\frac{1}{t}$. As described above, all hyperparameters are chosen to be the ones which minimize the aggregated KL score $\mathbf{d}_{\text{KL}}^{\text{agg}} = \mathbf{d}_{\text{KL}}^1 + \frac{1}{10} \mathbf{d}_{\text{KL}}^{10}$.

E.3 Results

Figures 8 and 9 shows the correlation between performance on testbed performance and sequential decision problems with an input dimension of 50. Different points of an agent in these figures corresponds to different random seeds for the testbed and sequential problems. We can see that performance on sequential decision problems is strongly correlated with testbed joint performance $\tau = 10$ and not correlated with the testbed marginal performance. In Figures 16 and 17 we show a similar correlation plots between testbed performance and sequential decision problems across different input dimensions for sequential decision problems. We can see that performance on sequential decision problems has clear correlation with testbed joint performance $\tau = 10$, and no correlation with testbed marginal performance $\tau = 1$, across all the input dimensions considered.

These results offer empirical evidence that practical deep learning approaches separated by the quality of their joint predictions, but not their marginals, can lead to differing performance in downstream tasks. In addition, we show that our simple 2D testbed can provide insights that scale to much higher dimension problems.

Algorithm 4 Evaluation on Bandit Problem

Require: Evaluation on bandit problem requires the following inputs

1. Distribution over the environment $\mathbb{P}(\mathcal{E} \in \cdot)$, input distribution P_X , and the number of actions N .
2. Agent f_θ
3. Number of time steps T
4. Number of sampled problems J

for $j = 1, 2, \dots, J$ **do**

Step 1: Sample environment and action set

1. Sample environment $\mathcal{E} \sim \mathbb{P}(\mathcal{E} \in \cdot)$
2. Sample a set \mathcal{X} of N actions x_1, x_2, \dots, x_N i.i.d. from P_X
3. Obtain the mean rewards corresponding to actions in \mathcal{X} conditioned on the environment

$$\bar{R}_x = \mathbb{P}(Y_{t+1} = 1 | \mathcal{E}, X_t = x), \quad \forall x \in \mathcal{X}$$

4. Compute the optimal expected reward $\bar{R}_* = \max_{x \in \mathcal{X}} \bar{R}_x$

Step 2: Agent interaction with the environment

 Initialize the data buffer $\mathcal{D}_0 = \{\}$

for $t = 1, 2, \dots, T$ **do**

1. Update agent f_{θ_t} belief distribution based on the data in the buffer \mathcal{D}_{t-1}
2. TS action selection scheme:
 - i. Sample $\hat{\mathcal{E}}_t$ from the agent belief distribution

$$\hat{\mathcal{E}}_t \sim \mathbb{P}(\hat{\mathcal{E}} \in \cdot | \theta_t)$$

- ii. Act greedily based on $\hat{\mathcal{E}}_t$

$$X_t \in \arg \max_{x \in \mathcal{X}} \mathbb{P}(\hat{Y}_{t+1} = 1 | \hat{\mathcal{E}}_t, X_t = x)$$

- iii. Generate observation Y_{t+1} based on action X_t

$$Y_{t+1} \sim \mathbb{P}(Y_{t+1} \in \cdot | \mathcal{E}, X_t = X_t)$$

3. Update the buffer $\mathcal{D}_t = \mathcal{D}_0 \cup (X_t, Y_{t+1})$

end for

 Compute the total regret incurred in T time steps

$$\text{Regret}_j(T) = \sum_{t=1}^T (\bar{R}_* - \bar{R}_{X_t})$$

end for

return $\frac{1}{J} \sum_{j=1}^J \text{Regret}_j(T)$

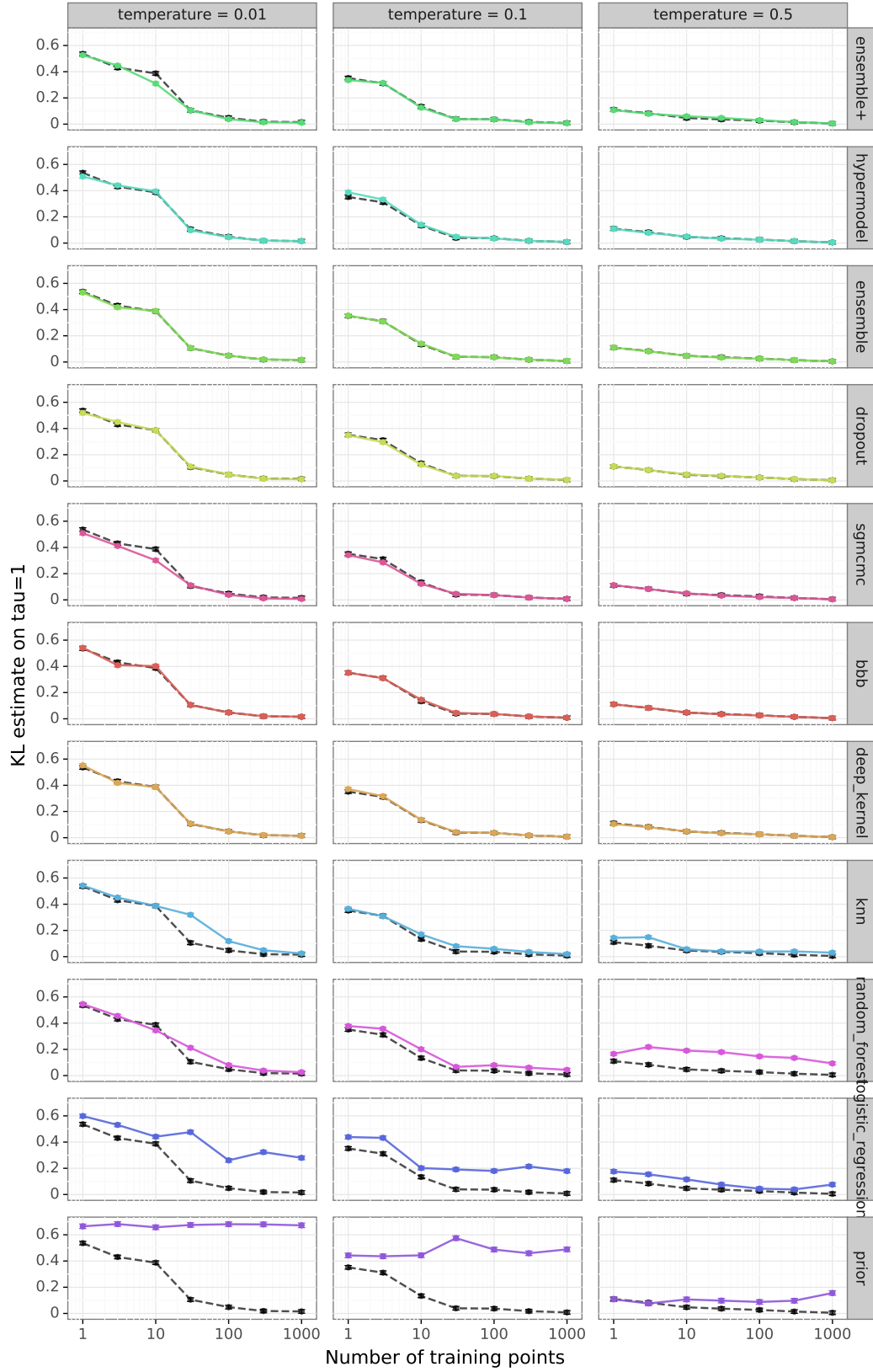


Figure 13: Performance of benchmark agents on the Testbed evaluated on $\tau = 1$, compared against the MLP baseline.

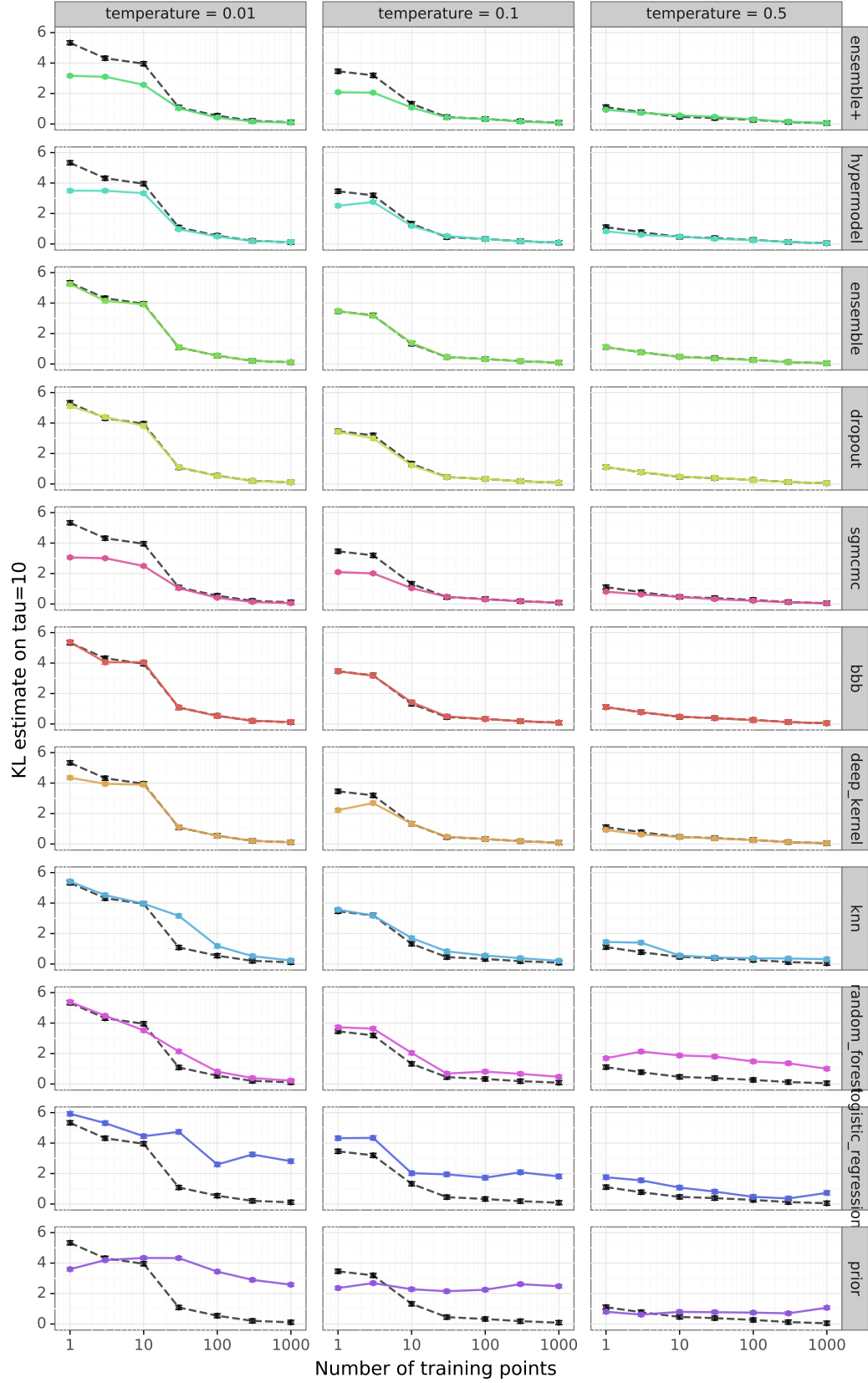


Figure 14: Performance of benchmark agents on the Testbed evaluated on $\tau = 10$, compared against the MLP baseline.

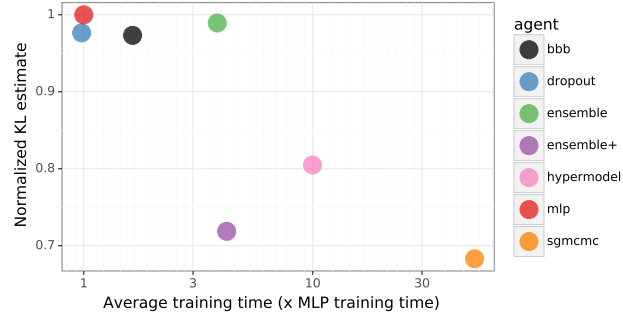


Figure 15: Normalized \mathbf{d}_{KL}^{10} vs training time of different agents

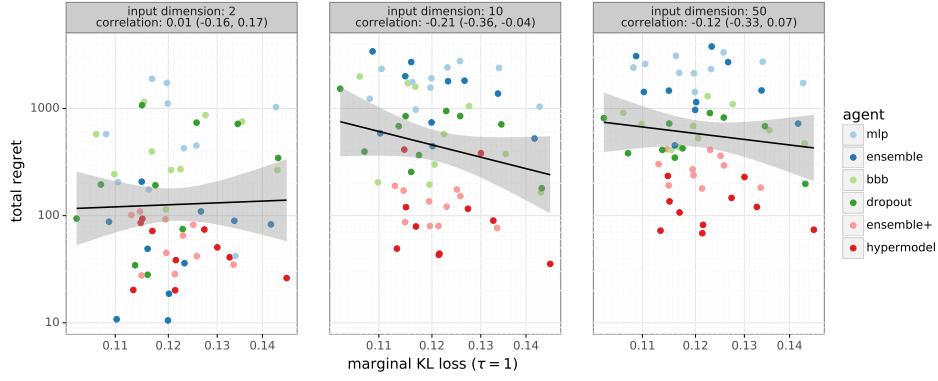


Figure 16: Testbed marginal performance \mathbf{d}_{KL}^1 is not significantly positively correlated with sequential decision performance. This result is robust across input dimensions 2, 10, and 50.

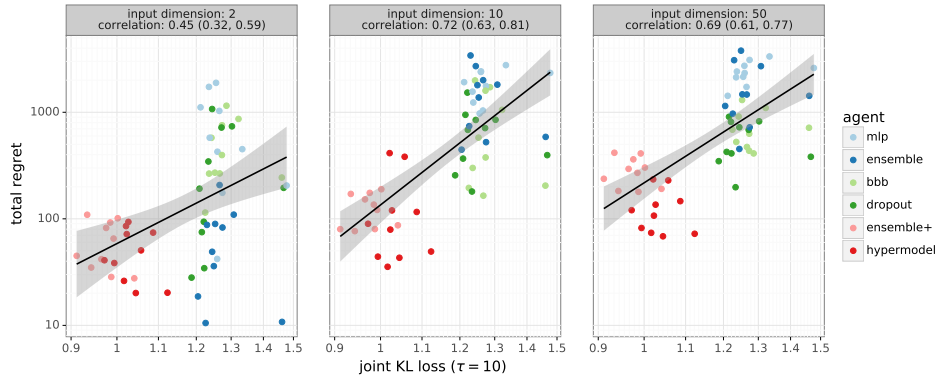


Figure 17: Testbed joint performance \mathbf{d}_{KL}^{10} is significantly positively correlated with sequential decision performance. This result is robust across input dimensions 2, 10, and 50.